Characterization of an in vitro model to study the possible role of polyomavirus BK in prostate cancer

Villani, Sonia ; Gagliano, Nicoletta ; Procacci, Patrizia ; Sartori, Patrizia ; Comar, Manola ; Provenzano, Maurizio ; Favi, Evaldo ; Ferraresso, Mariano ; Ferrante, Pasquale ; Delbue, Serena

Abstract: Prostate cancer (PCa) is the most common male neoplasms in the Western world. Various risk factors may lead to carcinogenesis, including infectious agents such as polyomavirus BK (BKPyV), which infects the human renourinary tract, establishes latency, and encodes oncoproteins. Previous studies suggested that BKPyV plays a role in PCa pathogenesis. However, the unspecific tropism of BKPyV and the lack of in vitro models of BKPyV-infected prostate cells cast doubt on this hypothesis. The aim of the present study was to determine whether BKPyV could (a) infect normal and/or tumoral epithelial prostate cells and (b) affect their phenotype. Normal epithelial prostate RWPE-1 cells and PCa PC-3 cells were infected with BKPyV for 21 days. Cell proliferation, cytokine production, adhesion, invasion ability, and epithelial-to-mesenchymal transition (EMT) markers were analyzed. Our results show that (a) RWPE-1 and PC-3 cells are both infectable with BKPyV, but the outcome of the infection varies, (b) cell proliferation and TNF- production were increased in BKPyV-infected RWPE-1, but not in PC-3 cells, (c) adhesion to matrigel and invasion abilities were elevated in BKPyV-infected RWPE-1 cells, and (d) loss of E-cadherin and expression of vimentin occurred in both uninfected and infected RWPE-1 cells. In conclusion, BKPyV may change some features of the normal prostate cells but is not needed for maintaining the transformed phenotype in the PCa cells The fact that RWPE-1 cells exhibit some phenotype modifications related to EMT represents a limit of this in vitro model.

DOI: https://doi.org/10.1002/jcp.27871

Characterization of an *in vitro* model to study the possible role of polyomavirus BK in prostate cancer

Running title: BK polyomavirus and prostate cancer

Sonia Villani[1*], Nicoletta Gagliano[2*], Patrizia Procacci[2], Patrizia Sartori[2], Manola Comar[3,4], Maurizio Provenzano[5], Evaldo Favi[6], Mariano Ferraresso[6], Pasquale Ferrante[1], Serena Delbue [1#]

[1]Department of Biomedical, Surgical and Dental Sciences, Università degli Studi di Milano, Italy

[2]Department of Biomedical Sciences for Health, Università degli Studi di Milano, Italy

[3]Institute for Maternal and Child Health - IRCCS "Burlo Garofolo," Trieste, Italy

[4]Department of Medical Sciences, University of Trieste, Trieste, Italy,

[5]Oncology Research Unit, Department of Urology and Division of Surgical Research, University and University Hospital of Zurich, CH-8091 Zurich, Switzerland

[6]Renal Transplantation Unit, Fondazione IRCCS Ca' Granda - Ospedale Maggiore Policlinico, Milan, Italy

* S. Villani and N. Gagliano should be considered joint first author

Acknowledgement

The study was supported by the Italian Ministry of University – PRIN 2015 to Pasquale Ferrante; contract grant number 2015w729wh. We thank Dott. Vincenzo Conte and Maria Dolci for skilful technical assistance in the EM and Western Blot, respectively, andMiss. Rosalia Ticozzi for technical help. The authors declare that they have no actual or potential competing financial interests.

#Corresponding Author:

Serena Delbue, PhD

Department of Biomedical, Surgical and Dental Sciences

Via Pascal, 36 - 20133 Milano – Italy, University of Milan

tel.+390250315070, serena.delbue@unimi.it

Abstract

Prostate cancer (PCa) is the most common male neoplasms in the Western world. Various risk factors may lead to carcinogenesis, including infectious agents such as polyomavirus BK (BKPyV), which infects the human renourinary tract, establishes latency, and encodes oncoproteins.

Previous studies suggested that BKPyV plays a role in PCa pathogenesis. However, the unspecific tropism of BKPyV and the lack of *in vitro* models of BKPyV-infected prostate cells cast doubt on this hypothesis.

The aim of the present study was to determine whether BKPyV could a) infect normal and/or tumoral epithelial prostate cells, and b) affect their phenotype. Normal epithelial prostate RWPE-1 cells and PCa PC-3 cells were infected with BKPyV for 21 days. Cell proliferation, cytokine production, adhesion, invasion ability, and epithelial-to-mesenchymal transition (EMT) markers were analyzed.

Our results show that a) RWPE-1 and PC-3 cells are both infectable with BKPyV, but the outcome of the infection varies, b) cell proliferation and TNF-α production were increased in BKPyV-infected RWPE-1, but not in PC-3 cells, c) adhesion to matrigel and invasion abilities were elevated in BKPyV-infected RWPE-1 cells, d) loss of E-cadherin and expression of vimentin occurred in both uninfected and infected RWPE-1 cells. In conclusion, BKPyV may change some features of the normal prostate cells, but is not needed for maintaining the transformed phenotype in the PCa cells The fact that RWPE-1 cells exhibit some phenotype modifications related to EMT represents a limit of this *in vitro* model.

Key words: Prostate Cancer, Polyomavirus, in vitro model, cytokine production

Introduction

Prostate cancer (PCa) is the most common malignant neoplasm in men and the second leading cause of cancer-related death in the Western world (NCI-NIH, 2018). Infectious agents such as human polyomavirus BK (BKPyV) should be considered as possible risk factors for PCa. BKPyV has been classified by the International Agency for Research on Cancer as "possibly" carcinogenic to humans due to evidence of carcinogenic activity *in vitro* in cell lines and *in vivo* in animals (Bouvard et al., 2012). The potential association between BKPyV and PCa is supported by previous studies, indicating that BKPyV infection is significantly more prevalent in cancer tissues than in control tissues, and that there is a significant association between viral expression and cancer (Delbue et al., 2014). However, the unspecific tropism of BKPyV and the lack of *in vitro* models of BKPyV infection in prostate cells cast doubt on this hypothesis.

The "phenotypic switch" from epithelial-to-mesenchymal, also referred to as the epithelial-to-mesenchymal transition (EMT) process, plays a pivotal role in PCa progression, because it makes tumor cells invasive and able to metastasize to distant organs. This EMT phenotype is characterized by loss of cell-cell adhesion and epithelial polarity markers (due to downregulation of E-cadherin), cytoskeleton reorganization (via expression of vimentin and α-smooth muscle actin), abnormal motile properties, and secretion of matrix metalloproteinases (MMPs) (Thiery, 2002).

The main goal of the present study was to determine whether BKPyV could infect normal and/or neoplastic prostate epithelial cells and whether this could affect cell morphology, proliferation, and adhesive properties, also focusing on EMT markers. For this purpose, we used normal human prostate epithelial cell line RWPE-1 and human PCa cell line PC-3.

Materials and methods

Cell cultures

The RWPE-1 (ATCC® CRL-11609) cell line was established from the epithelial cells of the peripheral zone of a normal adult human prostate, transfected with a single copy of human papillomavirus 18 (HPV-18). RWPE-1 cells were grown in a keratinocyte serum-free medium (K-SFM; GIBCO/Invitrogen, Karlsruhe, Germany) supplemented with 50 µg/mL recombinant human epidermal growth factor (rhEGF; GIBCO/Invitrogen, Karlsruhe, Germany), 5 ng/mL bovine pituitary extract (BPE; GIBCO/Invitrogen, Karlsruhe, Germany), and antibiotics (2.5 µg/mL Fungizone™; GIBCO/Invitrogen, Karlsruhe, Germany;50 U/mL penicillin; 50 µg/mL streptomycin; Euroclone, Italy). Human PCa cell line PC-3 (ATCC® CRL-1435) was derived from the grade IV prostate adenocarcinoma metastasis of a 62-year-old Caucasian patient. PC-3 cells were grown and subcultured in nutrient mixture Ham's F-12 Coon's modification medium with L-glutamine (Sigma-Aldrich, Germany) containing 10% v/v fetal bovine serum and antibiotics (50 U/mL penicillin; 50µg/mL streptomycin; Euroclone, Italy). All cells were maintained in an incubator at 37 °C in a 5% CO_2 humidified atmosphere.

BKPyV infection

Cells were infected using 10^8 virions corresponding to 4 X 10^6 virus DNA copies/mL (calculated by means of Real Time PCR) of BKPyV archetype (WW) strain stock, purchased at ATCC® (VR-837). The day before infection, 2 X 10^6 cells were plated in a T75 flask. On day 0, the cells (which reached 70% confluence) were washed twice with Dulbecco's phosphate-buffered saline w/o calcium and magnesium (DPBS; Euroclone, Italy) and then the virus stock, diluted with specific serum-free culture medium, was added to the flask. The cells were held at 37 °C for 90 min. Then, the inoculum was removed, the cells were washed with DPBS in order to eliminate the unbound virus, and the complete medium was added.

The uninfected control was created following the same procedure as for the infected cells but without the addition of the virus.

Infected and uninfected cells were continuously cultured with complete medium and were split every three days up to 21 days. Aliquots of cells and cell culture supernatants were collected for each splitting. Virions were precipitated from the culture medium using PEG-it Virus Precipitation Solution (PEG) (System Biosciences, USA) and then treated with DNase I; briefly, one part cold PEG (4 °C) was added to every four parts culture medium, refrigerated overnight, then processed according to the manufacturer's protocol. Supernatants were diluted 1:1 with nuclease-free water and treated with 5 U DNase I (5 U/µl) (AppliChem, Germany) or mock-treated with water. After 1 h at 37 °C, the enzyme was heat- inactivated at 99 °C for 10 min (Kantola et al., 2009).

BKPyV DNA isolation and quantitative real-time PCR

Viral DNA was isolated from the encapsidated virions and from the cell pellet using a Nucleospin RNA kit (Macherey-Nagel, Germany) and a QIAamp DNA blood mini kit (Qiagen, USA) according to the manufacturer's instructions. Titration and evaluation of extracellular and intracellular viral loads were carried out by BKPyV-specific quantitative real-time PCR (Q-PCR).

BKPyV Q-PCR assays were performed using a TaqMan chemistry with an Applied Biosystems 7500 Real-Time PCR System (Applied Biosystems, Carlsbad, CA), targeting the highly-conserved VP1 region according to a protocol previously described by Delbue and colleagues (Delbue et al., 2010) . A standard curve for quantification of the BKPyV viral load was obtained after serial dilution of the plasmid pBKPyV Dunlop with a dilution range between 10^0 and 10^8 plasmid copies/µL. Negative controls were included in each run and for each sample. Standards and controls were tested in triplicate. Data are expressed as viral copies/mL.

Western Blot

Western blot analyses targeting BKPyV VP1 (52 kDa), BKPyV LT-Ag proteins (80-94 kDa) and α tubulin protein (46-48 kDa) were performed on total protein lysates of BKPyV infected and uninfected RWPE-1 and PC-3 cells. As positive control, total protein lysate from BKPyV infected VERO cells was used. Cells were collected by scraping and were lysated by an incubation of 30 min at 4°C in constant agitation with ice-cold RIPA buffer (Pierce-Thermo Scientific, USA) added with 2X protease inhibitor (Halt™ Protease Inhibitor Single-Use Cocktail 100x, Pierce-Thermo Scientific, USA). After the incubation, the lysates were centrifuged at 4°C for 30 min at full speed. Proteins were separated by electrophoresis on 10% bis-tris polyacrylamide gels (Biorad) and transferred to a nitrocellulose membrane. Then, the nitrocellulose membrane was probed with anti-BKV VP1 (M02) mouse monoclonal antibody (cod MAB3204-M02, Abnova) diluted 1:1000, purified mouse monoclonal anti-SV40 LT-Ag (PAb416, cod ab16876, Abcam) diluted 1:50 in 5% Non-Fat Dry Milk in TBST and anti-α-tubulin (DM1A) mouse monoclonal Ab (cod. 3873; Cell Signaling Technology), diluted 1:8000 in 5% Non-Fat Dry Milk in TBST as control.

We used a horseradish peroxidase (HRP)-conjugated goat anti-mouse IgG antibody (Pierce-Thermo Scientific) diluted 1:5000 in 5% Non-Fat Dry Milk and the ECL kit (Advansta), to visualize proteins on an autoradiography film

Cell proliferation assay

The viability of infected and uninfected cells was measured by 3-[4,5-dimethylthiazol-2-yl]-2,5-diphenyltetrazolium bromide (MTT) assay. BKPyV-infected and uninfected cells were seeded in 96-well plates (5 X 10^4 cells per well) and cultured in complete medium at 37 °C and 5% CO_2 for 24 hours, 48 hours, 72 hours, and 6 days. At each time point, cells were washed with DPBS, and after addition of 100 µL MTT (Sigma-Aldrich, Germany), were left for 3 hours at 37 °C in the dark. Following incubation, the plate was centrifuged at 1200 rpm

for 10 min and then the medium was removed. Dimethyl sulfoxide (DMSO; Sigma-Aldrich, Germany) was added to each well to dissolve formazan product crystals, and the plate was shaken for 10 min in the dark Absorbance was measured using a BioTek Synergy™ 4 Hybrid Microplate Reader (Biotek, USA) at 550 nm. The background, read at 650 nm, was removed. Three replicates were made for each group. Cell viability was calculated as follows:

$$\text{Cell viability \%} = \frac{(\text{Absorbance of sample - Absorbance of blank})}{\text{Absorbance of negative control}} \times 100$$

Cytokine, chemokine, and growth factor analysis

Quantification of 48 different cytokines, chemokines, and growth factors (pro-human cytokine 27-Plex M50-0KCAF0Y and 21-Plex MF0-005KMII, Bio-Rad, Hercules, CA) was performed on the culture media of both BKPyV-infected and uninfected RWPE-1 and PC-3 cell lines when cells were split, by magnetic bead-based multiplex immunoassay (Bio-Plex®) (BIO-RAD Laboratories, Milano, Italy), according to manufacturer's instructions. We determined the presence and concentration of IL 1α-β-ra-2-2Ra-3-4-5-6-7-8-9-10-12p40 and p70-13-15-16-17-18, eotaxin, basic FGF, G-CSF, GM-CSF, IFN-γ, IP10, MCP1-α, MCP1-β, PDGFBB, RANTES, TNF-α, VEGF, CTACK, GRO-α, HGF, IFN-α2, LIF, MCP-3, M-CSF, MIF, MIG, β-NGF, SCF, SCGF-β, SDF1-α, TNF-β, TRAIL, ICAM1, and VCAM1. We used the Bio-Plex 200 reader and a digital processor for data acquisition and output. The Bio-Plex Manager® software presented data as median fluorescence intensity (MFI) and concentration (pg/mL) (BIO-RAD Laboratories, Milano, Italy), as described previously (Campisciano et al., 2018).

Matrigel cell adhesion

96-well plates were coated with 200 µL/cm^2 Cultrex® Basement Membrane Extract without phenol red (BME, PathClear®), a soluble form of basement membrane whose major components include laminin, collagen IV, entactin, and heparan sulfate proteoglycan. The plates were incubated at 37 °C for 30 min to allow polymerization of the matrix and the wells were washed with 1% bovine serum albumin in DPBS to block unspecified cell adhesion. Subsequently, infected and uninfected RWPE-1 and PC-3 cells were seeded at 5 X 10^4 cells per well and cultured in their specific complete media at 37 °C and 5% CO_2 for 60 min. A plastic plate was used as background control. Wells were washed with specific cell-type media to remove matrix non-adherent cells. The remaining adherent cells were fixed with 1% glutaraldehyde and counted microscopically. The mean cellular adhesion rate (adherent cells in coated wells - adherent cells in uncoated wells) was calculated considering three different observation fields using a phase-contrast microscope. The invasive characteristics of both cell lines were evaluated at days 4, 8, 15, and 21 post-infection, and compared with those of uninfected cells.

Immunofluorescence for EMT marker analysis

RWPE-1 and PC-3 cells were cultured on 12-mm diameter round coverslips in 24-well culture plates. Cells were washed in DPBS, fixed in 4% paraformaldehyde in DPBS containing 2% sucrose for 10 min at room temperature, post-fixed in 70% ethanol, and stored at -20 °C until use. Then, cells were washed in DPBS three times and incubated for 1 hour at room temperature with the primary antibodies anti-E-cadherin (1:2500, Becton Dickinson), anti-N-cadherin (1:200, Santa Cruz), anti-vimentin (1:200, Novocastra), and anti-αSMA (1:400, Sigma-Aldrich). Secondary antibodies conjugated with Alexa 488 (1:500, Molecular Probes, Invitrogen) were applied in DPBS for 1 h at room temperature in the dark. Negative controls were incubated in the same way, except for the primary antibody. Cells on coverslips were incubated for 15 min with DAPI (1:100.000, Sigma-Aldrich) and mounted onto glass

slides using Mowiol. Cells were photographed using a digital camera connected to a Nikon Eclipse microscope.

SDS-zymography for invasive potential analysis

Culture media were mixed 3:1 with sample buffer containing 10% SDS. Samples (10 µg total protein per sample) were run under non-reducing conditions without heat denaturation on 10% polyacrylamide gel (SDS-PAGE) co-polymerized with 1 mg/mL type I gelatin at 4 °C. After SDS-PAGE, gels were washed twice in 2.5% Triton X-100 for 30 min each and incubated overnight in a substrate buffer at 37 °C (Tris-HCl 50 mM, $CaCl_2$ 5 mM, NaN_3 0.02%, pH 7.5). After staining the gels with Coomassie Brilliant Blue R-250, MMP gelatinolytic activity was detected as clear bands on a blue background, quantified by densitometric scanning (UVBand, Eppendorf, Italy).

Tissue inhibitor of metalloproteinase-2 real-time PCR

Tissue inhibitor of metalloproteinase-2 (TIMP-2) gene expression was analysed by real-time PCR. Total RNA was isolated by a modified version of the acid guanidinium thiocyanate-phenol-chloroform method (Tri-Reagent, Sigma, Italy). 1 µg total RNA was reverse-transcribed in 20 µL (final volume) reaction mix (Biorad, Segrate-Milan, Italy). TIMP-2 mRNA levels were assessed and glyceraldehyde 3-phosphate dehydrogenase (GAPDH) was used as an endogenous control to normalize differences in the amount of total RNA in each sample. The primer sequence was sense CCCTTCATTGACCTCAACTACATG, antisense TGGGATTTCCATTGATGACAAGC for GAPDH and sense TGGAAACGACATTTATGGCAACCC, antisense CTCCAACGTCCAGCGAGACC for TIMP-2.

Amplification reactions were conducted in a 96-well plate in a final volume of 20 µL per well. Each well contained 10 µL 1X SYBR Green Supermix (BioRad, Italy), 2 µL template, and 300 pmol of each primer. Each sample was analysed in triplicate in a Bioer LineGene

9600. The cycle threshold was determined and gene expression levels relative to that of GAPDH were calculated.

Electronic microscopy for morphological analysis

RWPE-1 cells, grown at confluence, were harvested at 250 g for 5 min at room temperature. The culture medium was removed and replaced with a solution containing 2% freshly prepared paraformaldehyde and 2% glutaraldehyde in 0.1 M sodium cacodylate buffer (pH 7.4). Cells were fixed for 2–4 h at 4 °C, then were centrifuged and rinsed twice in cacodylate buffer for 20 min, post-fixed in 1% osmium tetroxide in the same buffer at 0 °C for 30 min, washed in distilled water, and *en bloc* stained with 2% aqueous uranyl acetate. After dehydration in a graded acetone series, samples were embedded in Epon-Araldite resin. Ultrathin sections (70–100 nm) were cut on a Leica Supernova ultramicrotome and stained with Reynolds' lead citrate. Transmission electron microscopy was performed with a Zeiss EM10 electron microscope.

Statistical analysis

All experiments were performed three to six times. Statistical significance was assessed using the Wilcoxon-Mann-Whitney U test. Differences were considered statistically significant at $p < 0.05$. Linear regression was performed for analysing changes in cytokine concentration over time.

Results

BKPyV infection – Viral DNA analysis

RWPE-1 and PC-3 cell lines were infected *in vitro* with a BKPyV archetype strain. Viral extracellular and intracellular DNA was quantified by specific Q-PCR at different time points postinfection. Both normal and cancerous epithelial prostate cell lines were found to be infectable with BKPyV, although a different time course of infection was observed in each cell line. Infection peaked on day 3 p.i. in RWPE-1 cells, with an extracellular viral load of

4.0 X 10^6 copies/mL and an intracellular viral load of 2.3 X 10^6 copies/mL. Viral replication was observed until day 14 p.i. (culture medium: undetectable; cell pellet: 7.7 X 10^2 copies/mL) (Figure 1A). In the PC-3 cell line, infection peaked on day 10 p.i., and the virus remained productive over 21 days p.i. with a mean extracellular viral load of 6.9 X 10^5 copies/mL (range: 8.7 X 10^3–2.6 X 10^6 copies/mL) and an intracellular viral load of 1.7 X 10^6 copies/mL (range: 2.4 X 10^5–3.9 X 10^6 copies/mL) (Figure 1B). Uninfected RWPE-1 and PC-3 did not harbour BKPyV genome or other DNA naked virus genomes (JC polyomavirus, SV40 polyomavirus, parvovirus, adenovirus), except for HPV-18, used for the immortalization of the RWPE-1 (data not shown).

BKPyV infection – protein expressions

Expression of BKPyV LT-Ag and VP1 proteins, as markers for early and late gene expression, respectively was examined in RWPE- 1 and PC-3 cells at 3,6 and 10 days p.i.. LT-Ag expression was detected at 10 days p.i. in RWPE-1 (Figure 2, panel A) and at all the analysed times p.i. in PC-3 cells (Fig. 2 panel B). VP1 expression was detected at 6 and 10 days p.i. in RWPE-1 (Figure 2, panel A), but was not detected in PC-3 at any analysed times p.i. (Figure 2, panel B)

BKPyV infection affects RWPE-1 cell proliferation

An MTT assay was performed on infected and uninfected cells to evaluate the effect of BKPyV infection on the growth rate of RWPE-1 and PC-3 cells. Infected cell viability was normalized to the viability of uninfected cells. Infected RWPE-1 cells showed a higher rate of proliferation compared to uninfected cells (range +25%/+58%, $p < 0.05$) (Figure 3A), whereas infected PC-3 cells displayed a significantly lower rate of proliferation than uninfected cells (range: -37%/-73%, $p < 0.05$) (Figure 3B).

BKPyV infection induces significant expression of inflammatory factors and activators in RWPE-1 cells

A panel of 48 cytokines and chemokines was analysed at seven time points p.i (24 and 48 hours; 3, 7, 12, 17, and 21 days) in the culture supernatants of infected and uninfected RWPE-1 and PC-3 cells (Table 1). The concentration of three factors involved in the tumor inflammatory microenvironment (IL-18, TNF-α, and MCP1) increased significantly in the supernatant of RWPE-1 infected cells compared to mock-infected counterparts (linear trend estimation: $R2 \geq 0.6$, $p \leq 0.04$; Figure 4A, B, and C). In particular, the concentration of the proinflammatory cytokine TNF-α in the supernatant of the RWPE-1 infected cells showed a linear increase from 1.13 pg/mL at hour 24 to 6.86 pg/mL on day 21 ($R^2 = 0.9$, $p < 0.0001$). This increase was much greater than in uninfected cells (on average 1.58 ± 0.18 pg/ml from 24 hours to 21 days). On the other end, the concentration of IL-3, a strong inducer of the active immune response, decreased significantly in the supernatant of infected RWPE-1 cells from 34.10 pg/ml at hour 24 to 6.58 pg/ml on day 21, compared to uninfected counterparts (4.77 to 48.05 pg/ml). The linear trend for IL-3 showed the significant effect of BKPyV infection on constitutive cytokine expression ($R^2 = 0.56$, $p < 0.05$) (Figure 4D). No significant linear trends were observed in the levels of cytokine/chemokine production between infected and uninfected PC-3 cells (table 1).

Matrigel adhesion assay

Both cell lines were seeded on BME, which mimics the extracellular matrix, to investigate the effect of BKPyV infection on the invasive behaviour of RWPE-1 and PC-3 cells. The binding rate of infected cells per mm^2 was calculated. Results were normalized to the binding rate of uninfected cells. Both infected cell lines showed a higher binding rate compared to their mock treated counterparts. The rate was from +17% to +1570% for RWPE-1 cells and from +9% to +811% for PC-3 cells (Figure 5, panels A and B).

EMT marker analysis

EMT marker expression was assessed by immunofluorescence in both infected and uninfected RWPE-1 cells. At all time points, uninfected RWPE-1 cells exhibited low or undetectable levels of E-cadherin. Immunoreactivity was observed mostly in the cytoplasm and not in cell boundaries, in which functional adherent junctions are located in normal differentiated epithelial cells. Infected RWPE-1 cells showed a similar pattern of E-cadherin expression. N-cadherin expression was almost undetectable, with scattered positive cells in both infected and uninfected RWPE-1 cells. Vimentin expression was similar in infected and uninfected RWPE-1 cells (Figure 6, panel A).

To better investigate the effect of BKPyV on normal epithelial cells and its possible involvement in PCa oncogenesis, the expression of EMT markers was analysed in PC-3 cells before and after BKPyV infection. As expected, E-cadherin was almost completely undetectable in both infected and uninfected PC-3 cells at all time points. N-cadherin and vimentin expression were similarly expressed in control and BKPyV-infected PC-3 cells (Figure 6, panel B).

Invasive potential

To determine the invasive potential of infected and uninfected RWPE-1 and PC-3 cells, MMP-2 and MMP-9 gelatinolytic activity in cell supernatants was assessed by SDS-zymography. Densitometric scanning of lytic bands on zymograms revealed that MMP-2 and MMP-9 were similarly expressed in uninfected and infected RWPE-1 cells up to day 3. At all subsequent time points, MMP-2 and MMP-9 were strongly induced in BKPyV-infected cells compared to uninfected cells (Figure 7, panel A and B).

Densitometric analysis of lytic bands also showed that the activity of MMP-2 and MMP-9 in PC-3 cells were differently affected by BKPyV infection in a time-dependent manner that could not be properly defined (data not shown). To assess whether the invasive potential of PC-3 cells was influenced by BKPyV infection, we analysed the expression of TIMP-2, a

natural inhibitor of MMP-2, and described MMP-2 and MMP-9 activity in relation to TIMP-2 expression. The MMP-2:TIMP-2 ratio was strongly increased by BKPyV from day 3 to day 14, and thereafter, was similar to that in control cells. A comparable pattern was observed in the MMP-9:TIMP-2 ratio (Figure 7, panel C).

Morphological analysis by electron microscopy

The morphology and ultrastructure of infected and uninfected RWPE-1 cells at different time points were analysed by electron microscopy. For each pellet, 120 cells were photographed and evaluated to observe the presence of any viral particles. Both uninfected and infected cells showed similar morphologies (Figure 8, panel A) and contained a high number of viral particles (Figure 8, panel B). Unexpectedly, viral particles were observed in both infected and uninfected RWPE-1 cells, although BKPyV DNA and proteins were undetectable by Q-PCR and western blot, respectively.

Discussion

BKPyV is a member of the *Polyomaviridae* family with very well-known *in vitro* oncogenic properties, mainly resulting from the production of the large T antigen protein, which is able to induce cell transformation (Tognon et al., 2003). Based on serological and molecular studies, it has been suggested that BKPyV may be involved in the etiology and/or development of PCa (Delbue et al., 2014; Keller et al., 2015). However, it remains uncertain whether BKPyV infection is a causative agent in PCa or an epiphenomenon. The lack of an *in vitro* model of BKPyV-infected epithelial prostate cells represents a major limitation.

In the present study, we infected prostate cells with BKPyV with the aim of establishing and characterizing an *in vitro* model to obtain further insight into the relationship between viral activity and possible phenotypic changes.

We demonstrated for the first time that both normal epithelial prostate cell line RWPE-1 and PCa cell line PC-3 are infectable with BKPyV. Moreover, we showed that the outcomes of

the infection varies in the two cell lines, being the viral DNA lost from RWPE-1 by day 14 p.i., but persisting in PC-3 up to three weeks p.i. BKPyV was capable of expressing early and late proteins LT-Ag and VP1 within RWPE-1, but only LT-Ag in PC-3. These findings suggest that normal prostate cells are subjected to a transient infection. On the other hand, PC-3 cells seem to maintain a steady state of BKPyV replication over time, limiting protein expression to early LT-Ag. Therefore, it is plausible that a persistent infection was established in PC-3 cells.

Our results are difficult to compare with those from other studies, as previous experiments on BKPyV infection *in vitro* have been performed in human or monkey kidney cells, lung fibroblasts, or epithelial cells from salivary glands (Acott et al., 2006; Jeffers-Francis et al., 2015; Li et al., 2013). Despite the quick lost of the infection, BKPyV seems to affect some of the properties of normal prostate cells, such as their proliferation rate and the production of factors possibly involved in malignant transformation.

TNF-α is a pleiotropic cytokine that can induce cancer cell death, but may also favor cell proliferation under certain specific conditions (Tse et al., 2012). In addition, TNF-α orchestrates the expression of inflammatory cytokines involved in the development of castrate-resistant PCa, such as IL-6 (Nguyen et al., 2014). Interestingly, TNF-α showed a strong growth-stimulating effect on simian polyomavirus 40-transformed keratinocytes (Kobayashi et al., 1999), and a similar effect on BKPyV-infected prostate cells can be hypothesized, upon synergic stimulation of proliferation with viral LT-Ag.

The concomitant upregulation of TNF-α, IL-18, and MPC-1 upon BKPyV infection might contribute to the promotion of prostatic cells toward a cancerous phenotype (Ito et al., 2015; Palma et al., 2013). In addition, the role of IL-18 as a potent inducer of IFN-γ, suggests a relevant role of BKPyV in PCa development and progression (Feder-Mengus et al., 2008).

Finally, the inhibition of IL-3 production should help BKPyV evade the host innate immune response (Broughton et al., 2012).

On the contrary, infected PC-3 cells showed a decrease in their proliferation rate, probably due to the cytopathic effect and stable expression of TNF-α after BKPyV infection.

We evaluated the binding of BKPyV-infected RWPE-1 and PC-3 cells to the extracellular matrix because direct interaction with the extracellular matrix may lead to transendothelial invasion. BKPyV-infected cells showed higher adhesion to Matrigel than uninfected cells, even though there was no specific trend over time. Further comparison demonstrated that infected PC3 cells had more adhesion capability than infected RWPE-1. The inverse relationship between E-cadherin expression and adhesion to Matrigel was previously described by Jannesari-Ladani et al. who suggested a more destabilized E-cadherin-based adhesion in PC-3 cells (Jannesari-Ladani et al., 2014).

Higher levels and activity of MMP-2 and MMP-9 in BKPyV-infected RWPE-1 showed that the virus elicited an invasive phenotype in normal cells. Increased expression of MMP-2 and, consequently, strong invasive behavior of the cells has previously been described in a transgenic mouse model with polyomavirus-induced osteosarcoma (Velupillai et al., 2010). Very recently, the induction of several MMPs has been described in an *in vitro* model of Merkel cell carcinoma induced by Merkel cell polyomavirus; the authors hypothesized that dysregulated MMP gene expression may contribute to virus-induced oncogenesis (Liu et al., 2016). Both enhanced cell adhesion to the extracellular matrix and increased activity of MMP-2 and MMP-9 have been observed even after clearance of the BKPyV genome from the RWPE-1 cells.

The increased levels and activity of MMPs induced by BKPyV in PC-3 cells suggests that the viral DNA replication was effective in adding invasive potential to already established invasive properties.

Although all the above evidence could reasonably lead to the hypothesis that BKPyV catalyses some changes in RWPE-1 cells, we observed an unexpected result regarding EMT markers and the EMT-related phenotype. Uninfected RWPE-1 cells are normal epithelial cells, but our data shows that they do not present a clear epithelial phenotype; E-cadherin downregulation and cytoplasmic localization was detected in most cells, and vimentin expression was observed in both control and BKPyV-infected cells, thus suggesting that uninfected cells underwent EMT. This finding was consistent with the morphological results in the same cells as described by Tam and colleagues. (Tam et al., 2017). To better understand this unexpected result, we analyzed RWPE-1 cells by electron microscope. Small viral particles were detected not only in BKPyV-infected cells, but also in normal, uninfected RWPE-1 prostate cells, although BKPyV viral DNA and proteins were undetectable, suggesting that these viral particles were a result of HPV-18 used for RWPE-1 immortalization.

It is likely that RWPE-1 cells, which have been immortalized with a defective HPV-18 genome, are still able to produce viral capsid proteins (known as L1), which spontaneously self-assemble into a structure closely mimicking the natural surface of native papillomavirus virions (Buck et al., 2013). The concomitant presence of these pseudovirions and the observation of an EMT-related phenotype in uninfected RWPE-1 cells strongly suggests that RWPE-1 cells do not retain a normal epithelial morphology (Bello et al., 1997) and may not serve as a model of normal epithelial prostate cells, even if they are used for research purpose (Deng et al., 2017; Souza et al., 2018). BKPyV-infected and uninfected RWPE-1 cells exhibit a similar EMT phenotype, suggesting that uninfected cells do not retain normal epithelial characteristics and thus their use as a model of normal epithelial prostate cells may be limited. However, under our experimental conditions, we were able to demonstrate that BKPyV infection induced increased gelatinolytic activity in RWPE-1 cells, allowing us to

detect the effect of BKPyV in inducing the invasive properties of infected cells, consistent with their malignant transformation. Previous reports have described aberrant expression of E-cadherin and vimentin in normal prostate tissues (Figiel et al., 2017; Rubin et al., 2001), indicating that further research is necessary to understand whether the EMT morphological features of untreated RWPE-1 cells are induced by HPV and validate the use of these cells as an experimental model for normal prostate epithelial cells.

As expected, PC-3 carcinoma cells were characterized by an EMT phenotype and no additional morphological modifications were induced by BKPyV infection. In contrast, BKPyV infection increased their invasive potential.

Considered as a whole, our results show that a) normal epithelial prostate RWPE-1 cells and PC-3 cells are infectable with BKPyV, but the outcomes of infection vary, b) cell proliferation and TNF-α production were increased by BKPyV in RWPE-1 cells, but not in PC-3 cells, c) adhesion to Matrigel and invasion potential, observed as MMP-2 and MMP-9 activities, were increased upon BKPyV infection of RWPE-1 cells, d) both mock treated and BKPyV-infected RWPE-1 cells exhibit loss of E-cadherin and expression of vimentin.

In conclusion, we hypothesize that BKPyV may establish a transient infection in normal epithelial prostate cells and change some phenotypic features, such as the proliferation, adhesion and invasive potential, but then it is not needed for maintaining the transformed phenotype of prostate tumor cells. However, the fact that mock treated RWPE-1 cells exhibit some phenotype modifications related to EMT represents a limit of this *in vitro* model.

Table 1: Cytokine and chemokine concentration trends in BKPyV-infected RWPE-1 and PC-3 cells

Cytokine/chemokine	*Linear trend estimation*,***	
	RWPE-1	**PC-3**
IL-18	**R^2 0.69; p=0.02**	R^2 0.89; p=0.09
TNF-α	**R^2 0.85; p<0.01**	R^2 0.61; p=0.80
MCP1	**R^2 0.59; p=0.04**	R^2 0.86; p=0.17
IL-15	R^2 0.24; p=0.26	n.a.
IL-2	R^2 0.4; p=0.12	R^2 0.13; p=0.26
IL-6	R^2 0.03; p=0.71	R^2 0.80; p=0.42
IL-9	R^2 0.07; p=0.55	R^2 0.20; p=0.07
GM-CSF	R^2 0.3; p=0.1	R^2 0.39; p=0.4
FGF-basic	R^2 0.21; p=0.29	R^2 0.99; p=0.12
MIP-1a	R^2 0.26; p=0.24	R^2 0.59; p=0.06
MIP-1b	R^2 0.04; p=0.95	R^2 0.01; p=0.60
IL-3	**R^2 0.56; p=0.05**	R^2 0.96; p=0.36
M-CSF	R^2 0.03; p=0.70	R^2 0.74; p=0.66
SDF-1	R^2 0.29; p=0.20	R^2 0.89; p=0.64

**compared to uninfected RWPE-1 cells*

***from 1 to 21 days p.i.*

References

Acott PD, O'Regan PA, Lee SH, Crocker JF. 2006. Utilization of vero cells for primary and chronic BK virus infection. Transplant Proc 38(10):3502-3505.

Bello D, Webber MM, Kleinman HK, Wartinger DD, Rhim JS. 1997. Androgen responsive adult human prostatic epithelial cell lines immortalized by human papillomavirus 18. Carcinogenesis 18(6):1215-1223.

Bouvard V, Baan RA, Grosse Y, Lauby-Secretan B, El Ghissassi F, Benbrahim-Tallaa L, Guha N, Straif K. 2012. Carcinogenicity of malaria and of some polyomaviruses. Lancet Oncol 13(4):339-340.

Broughton SE, Dhagat U, Hercus TR, Nero TL, Grimbaldeston MA, Bonder CS, Lopez AF, Parker MW. 2012. The GM-CSF/IL-3/IL-5 cytokine receptor family: from ligand recognition to initiation of signaling. Immunol Rev 250(1):277-302.

Buck CB, Day PM, Trus BL. 2013. The papillomavirus major capsid protein L1. Virology 445(1-2):169-174.

Campisciano G, Zanotta N, Licastro D, De Seta F, Comar M. 2018. In vivo microbiome and associated immune markers: New insights into the pathogenesis of vaginal dysbiosis. Sci Rep 8(1):2307.

Delbue S, Ferrante P, Provenzano M. 2014. Polyomavirus BK and prostate cancer: an unworthy scientific effort? Oncoscience 1(4):296-303.

Delbue S, Tremolada S, Elia F, Carloni C, Amico S, Tavazzi E, Marchioni E, Novati S, Maserati R, Ferrante P. 2010. Lymphotropic polyomavirus is detected in peripheral blood from immunocompromised and healthy subjects. J Clin Virol 47(2):156-160.

Deng G, Zheng X, Jiang P, Chen K, Wang X, Jiang K, Zhang W, Tu L, Yan D, Ma L, Ma S. 2017. Notch1 suppresses prostate cancer cell invasion via the metastasis-associated 1-KiSS-1 metastasis-suppressor pathway. Oncol Lett 14(4):4477-4482.

Feder-Mengus C, Wyler S, Hudolin T, Ruszat R, Bubendorf L, Chiarugi A, Pittelli M, Weber WP, Bachmann A, Gasser TC, Sulser T, Heberer M, Spagnoli GC, Provenzano M. 2008. High expression of indoleamine 2,3-dioxygenase gene in prostate cancer. Eur J Cancer 44(15):2266-2275.

Figiel S, Vasseur C, Bruyere F, Rozet F, Maheo K, Fromont G. 2017. Clinical significance of epithelial-mesenchymal transition markers in prostate cancer. Hum Pathol 61:26-32.

Ito Y, Ishiguro H, Kobayashi N, Hasumi H, Watanabe M, Yao M, Uemura H. 2015. Adipocyte-derived monocyte chemotactic protein-1 (MCP-1) promotes prostate cancer progression through the induction of MMP-2 activity. Prostate 75(10):1009-1019.

Jannesari-Ladani F, Hossein G, Monhasery N, Shahoei SH, Izadi Mood N. 2014. Wnt5a influences viability, migration, adhesion, colony formation, E- and N-cadherin expression of human ovarian cancer cell line SKOV-3. Folia Biol (Praha) 60(2):57-67

Jeffers-Francis LK, Burger-Calderon R, Webster-Cyriaque J. 2015. Effect of Leflunomide, Cidofovir and Ciprofloxacin on replication of BKPyV in a salivary gland in vitro culture system. Antiviral Res 118:46-55.

Kantola K, Sadeghi M, Lahtinen A, Koskenvuo M, Aaltonen LM, Mottonen M, Rahiala J, Saarinen-Pihkala U, Riikonen P, Jartti T, Ruuskanen O, Soderlund-Venermo M, Hedman K. 2009. Merkel cell polyomavirus DNA in tumor-free tonsillar tissues and upper respiratory tract samples: implications for respiratory transmission and latency. J Clin Virol 45(4):292-295.

Keller EX, Delbue S, Tognon M, Provenzano M. 2015. Polyomavirus BK and prostate cancer: a complex interaction of potential clinical relevance. Rev Med Virol 25(6):366-378.

Kobayashi T, Okumura H, Hashimoto K, Asada H, Yoshikawa K. 1999. Growth-stimulating effects of tumor necrosis factor-alpha on simian virus 40-transformed human keratinocytes is linked to phosphorylation of retinoblastoma protein. J Dermatol Sci 22(1):38-44.

Li R, Sharma BN, Linder S, Gutteberg TJ, Hirsch HH, Rinaldo CH. 2013. Characteristics of polyomavirus BK (BKPyV) infection in primary human urothelial cells. Virology 440(1):41-50.

Liu W, Yang R, Payne AS, Schowalter RM, Spurgeon ME, Lambert PF, Xu X, Buck CB, You J. 2016. Identifying the Target Cells and Mechanisms of Merkel Cell Polyomavirus Infection. Cell Host Microbe 19(6):775-787.

NCI-NIH. 2018. Cancer Stat Facts https://seer.cancer.gov/statfacts/html/prost.html.

Nguyen DP, Li J, Tewari AK. 2014. Inflammation and prostate cancer: the role of interleukin 6 (IL-6). BJU Int 113(6):986-992.

Palma G, Barbieri A, Bimonte S, Palla M, Zappavigna S, Caraglia M, Ascierto PA, Ciliberto G, Arra C. 2013. Interleukin 18: friend or foe in cancer. Biochim Biophys Acta 1836(2):296-303.

Rubin MA, Mucci NR, Figurski J, Fecko A, Pienta KJ, Day ML. 2001. E-cadherin expression in prostate cancer: a broad survey using high-density tissue microarray technology. Hum Pathol 32(7):690-697.

Souza AG, B Silva IB, Campos-Fernández E, Marangoni K, F Bastos VA, Alves PT, Goulart LR, Alonso-Goulart V. 2018. Extracellular vesicles as drivers of epithelial-mesenchymal transition and carcinogenic characteristics in normal prostate cells. Mol Carcinog 57(4):503-511.

Tam KJ, Hui DHF, Lee WW, Dong M, Tombe T, Jiao IZF, Khosravi S, Takeuchi A, Peacock JW, Ivanova L, Moskalev I, Gleave ME, Buttyan R, Cox ME, Ong CJ. 2017. Semaphorin 3 C drives epithelial-to-mesenchymal transition, invasiveness, and stem-like characteristics in prostate cells. Sci Rep 7(1):11501.

Thiery JP. 2002. Epithelial-mesenchymal transitions in tumour progression. Nat Rev Cancer 2(6):442-454.

Tognon M, Corallini A, Martini F, Negrini M, Barbanti-Brodano G. 2003. Oncogenic transformation by BK virus and association with human tumors. Oncogene 22(33):5192-5200.

Tse BW, Scott KF, Russell PJ. 2012. Paradoxical roles of tumour necrosis factor-alpha in prostate cancer biology. Prostate Cancer 2012:128965.

Velupillai P, Sung CK, Tian Y, Dahl J, Carroll J, Bronson R, Benjamin T. 2010. Polyoma virus-induced osteosarcomas in inbred strains of mice: host determinants of metastasis. PLoS Pathog 6(1):e1000733.

Figure captions

Figure 1: Titration of BKPyV load, expressed as copies/mL, in RWPE-1 (Panel A) and PC-3 (Panel B) culture media and cell pellets, at every analyzed time points, from day 1 to day 21 p.i..

Figure 2: Expression of BKV early and late proteins in RWPE-1 (Panel A) and PC-3 (Panel B) cells. Total cellular protein isolated at the indicated times p.i. (3,6 and 10 days) was analyzed as described in Metarials and methods section. As negative control (C-), total protein isolated from uninfected RWPE- 1 or PC-3 cells was used; as positive control (C+), total protein isolated from BKPyV infected VERO cells was used.

Figure 3: Effect of BKPyV infection on the growth rate of RWPE-1 (Panel A) and PC-3 (Panel B) cells measured by the MTT assay. Data are expressed as percentage of the cell viability, compared to the uninfected cells (100%).

Figure 4: Concentration of four most significant cytokines (Panel A: IL-18; panel B: TNF-α; panel C: MCP1; and panel D: IL-3), measured in the culture medium of the infected and uninfected RWPE-1 cells, at every analyzed time points, from day 1 to day 21 p.i. Data are expressed as pg/mL and as percentage of increase. Linear trend estimation is indicated for every cytokines.

Figure 5: Panel A and B represent the percentage of adhesion rate to the extracellular matrix of the BKPyV infected RWPE-1 and PC-3, respectively, at different time points, from 4 to 21 days p.i.. Adhesion capacity is depicted as percentage of cell adhesion/square millimeter (mean± SD), compared to uninfected cells (100%).

Figure 6: Panel A) Representative micrographs at the fluorescence microscope showing the expression of epithelial and mesenchymal markers in control and BKPyV-infected RWPE-1 cells 7 days p.i. (original magnification 60x). Panel B) Representative micrographs at the fluorescence microscope showing the expression epithelial and mesenchymal markers in control and BKPyV-infected PC-3 cells 21 days p.i. (original magnification 60x).

Figure 7: Panel A) Representative gelatin zymogram and bar graphs showing MMP-2 (panel B) and MMP-9 (panel C) activity in supernatants of cultured control and BKPyV-infected RWPE-1 cells. Data are expressed as mean ± SD. Representative gelatin zymogram and bar graphs showing MMP-/TIMP-2 (panel D) ratio and MMP-9/TIMP-2 ratio (panel E) activity in supernatants of cultured control and BKPyV-infected PC3 cells. Data are expressed as mean ± SD.

Figure 8: Panel A) Transmission electron micrographs of RWPE-1 non infected (a) and BKPyV-infected-RWPE-1 (b) cells at 3 days showing a similar morphology. Scale bars = 0,5 µm. Boxed areas show at higher magnification the viral particles present in both experimental conditions. Scale bars = 200 nm. Panel B) Transmission electron micrographs of RWPE-1 non infected (c) and BKPyV-infected-RWPE-1 (d) cells at 10 days p.i. containing viral particles (some indicated by white arrows). Scale bars = 0,5 µm. A viral particle from each experimental condition is shown at higher magnification in boxed areas. Scale bars = 120 nm.

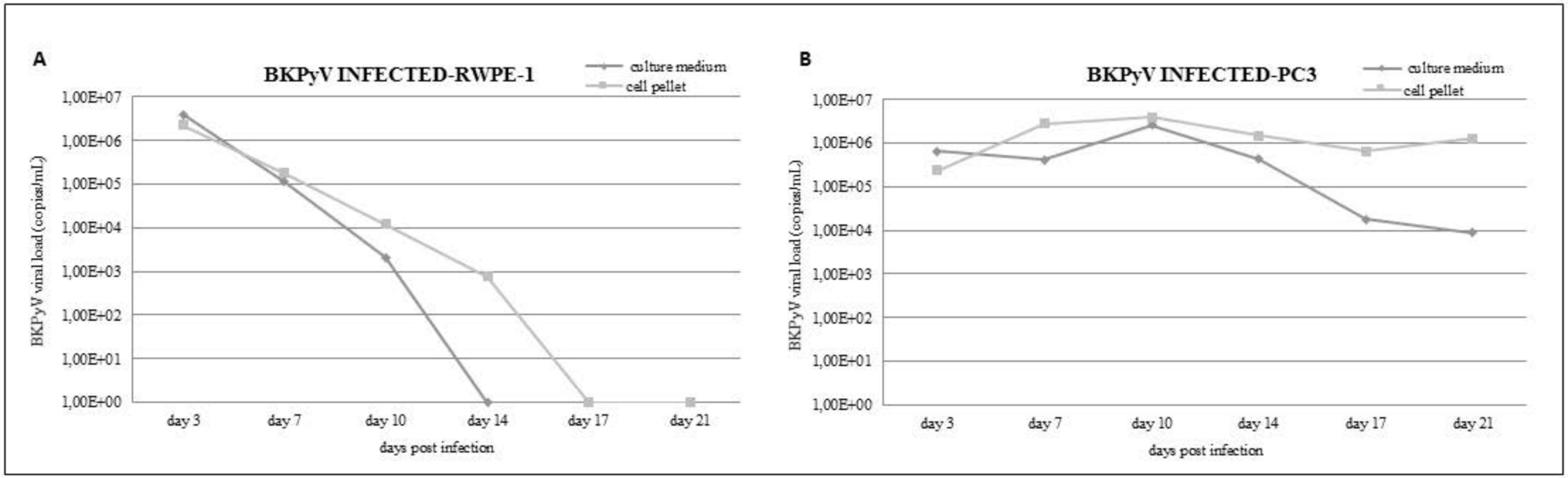
A
BKPyV INFECTED-RWPE-1
culture medium
cell pellet
1,00E+07
1,00E+06
1,00E+05
1,00E+04
1,00E+03
1,00E+02
1,00E+01
1,00E+00
BKPyV viral load (copies/mL)
day 3
day 7
day 10
day 14
day 17
day 21
days post infection
B
BKPyV INFECTED-PC3
culture medium
cell pellet
1,00E+07
1,00E+06
1,00E+05
1,00E+04
1,00E+03
1,00E+02
1,00E+01
1,00E+00
BKPyV viral load (copies/mL)
day 3
day 7
day 10
day 14
day 17
day 21
days post infection

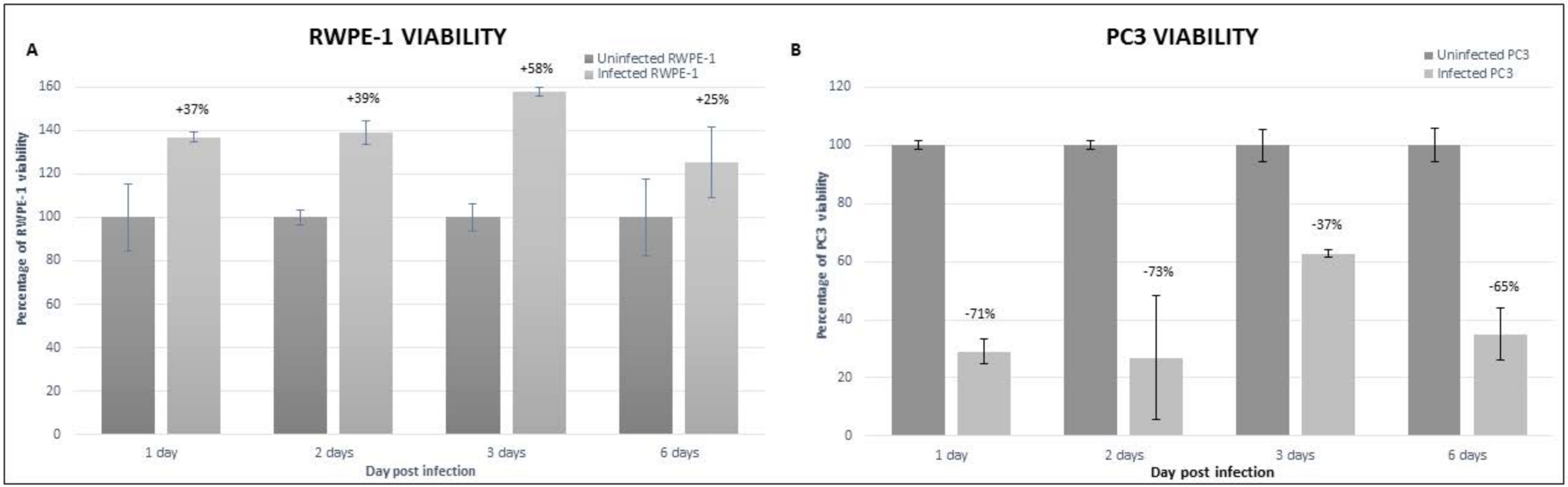
A
RWPE-1 VIABILITY
Uninfected RWPE-1
Infected RWPE-1
Percentage of RWPE-1 viability
160
140
120
100
80
60
40
20
0
+37%
+39%
+58%
+25%
1 day
2 days
3 days
6 days
Day post infection
B
PC3 VIABILITY
Uninfected PC3
Infected PC3
Percentage of PC3 viability
120
100
80
60
40
20
0
-71%
-73%
-37%
-65%
1 day
2 days
3 days
6 days
Day post infection

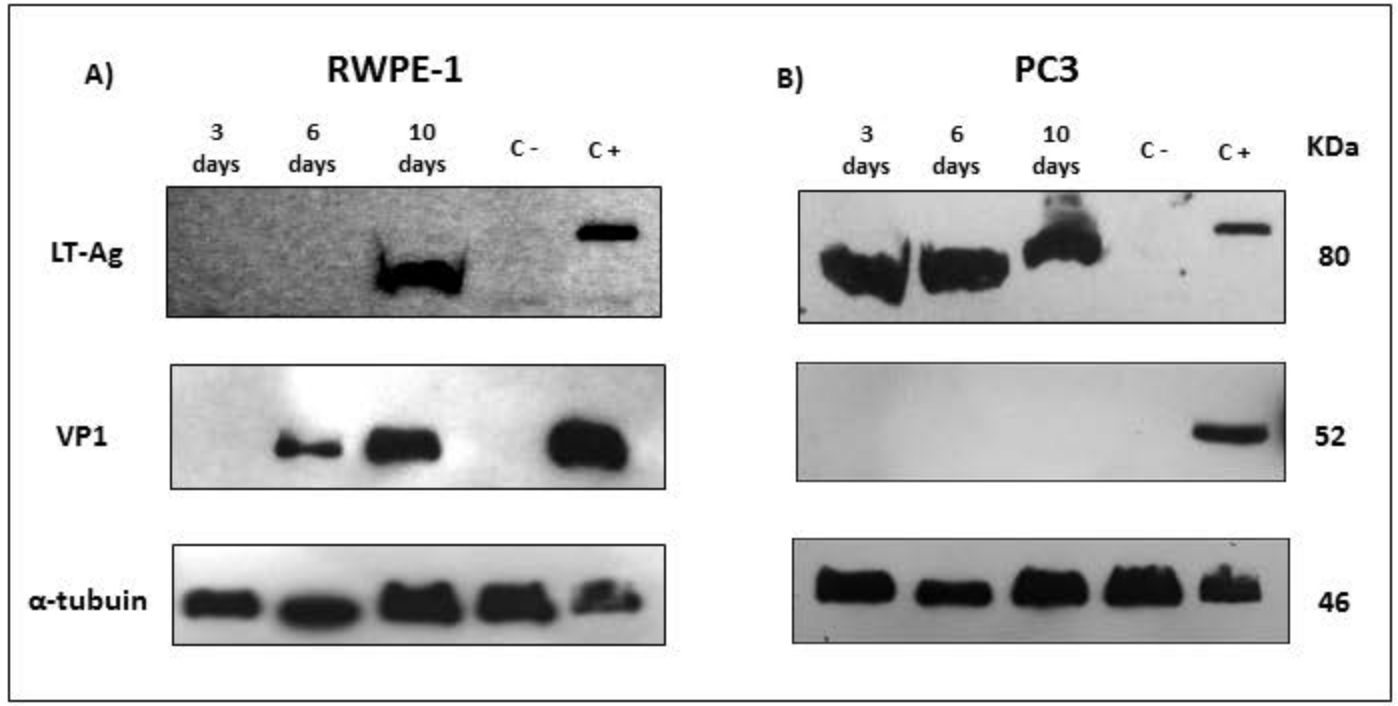
A)
RWPE-1
3 days
6 days
10 days
C -
C +
LT-Ag
VP1
α-tubuin
B)
PC3
3 days
6 days
10 days
C -
C +
KDa
80
52
46

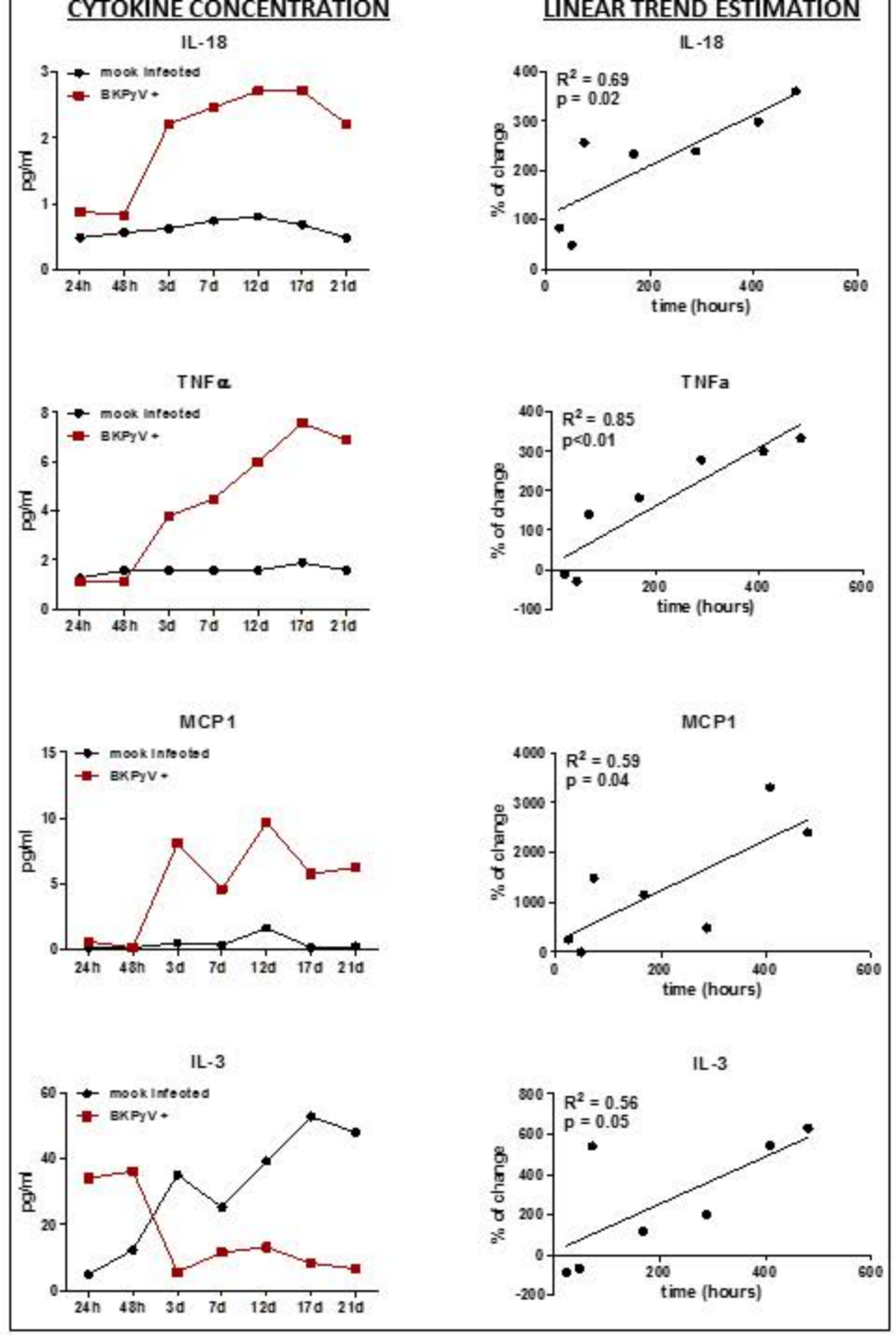
CYTOKINE CONCENTRATION
LINEAR TREND ESTIMATION
IL-18
mock infected
BKPyV +
pg/ml
24h 48h 3d 7d 12d 17d 21d
IL-18
R² = 0.69
p = 0.02
% of change
time (hours)
TNFα
mock infected
BKPyV +
pg/ml
24h 48h 3d 7d 12d 17d 21d
TNFa
R² = 0.85
p<0.01
% of change
time (hours)
MCP1
mock infected
BKPyV +
pg/ml
24h 48h 3d 7d 12d 17d 21d
MCP1
R² = 0.59
p = 0.04
% of change
time (hours)
IL-3
mock infected
BKPyV +
pg/ml
24h 48h 3d 7d 12d 17d 21d
IL-3
R² = 0.56
p = 0.05
% of change
time (hours)

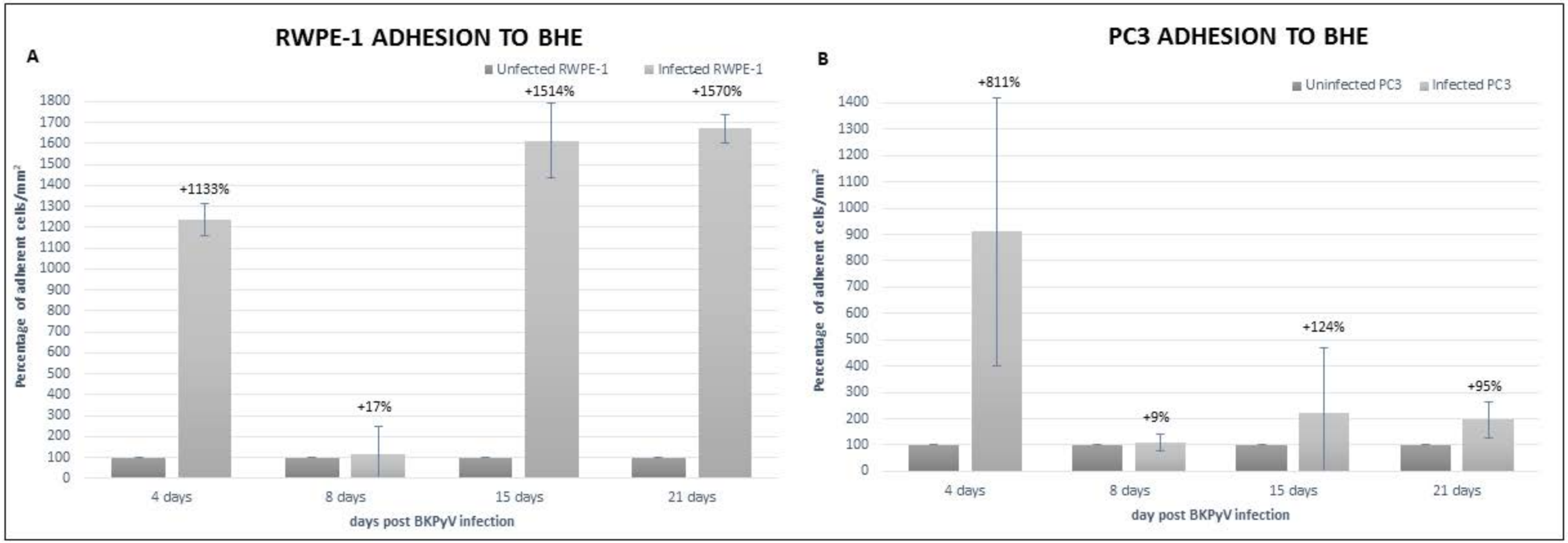
A
RWPE-1 ADHESION TO BHE
Unfected RWPE-1
Infected RWPE-1
Percentage of adherent cells/mm²
+1133%
+17%
+1514%
+1570%
4 days
8 days
15 days
21 days
days post BKPyV infection
B
PC3 ADHESION TO BHE
Uninfected PC3
Infected PC3
Percentage of adherent cells/mm²
+811%
+9%
+124%
+95%
4 days
8 days
15 days
21 days
day post BKPyV infection

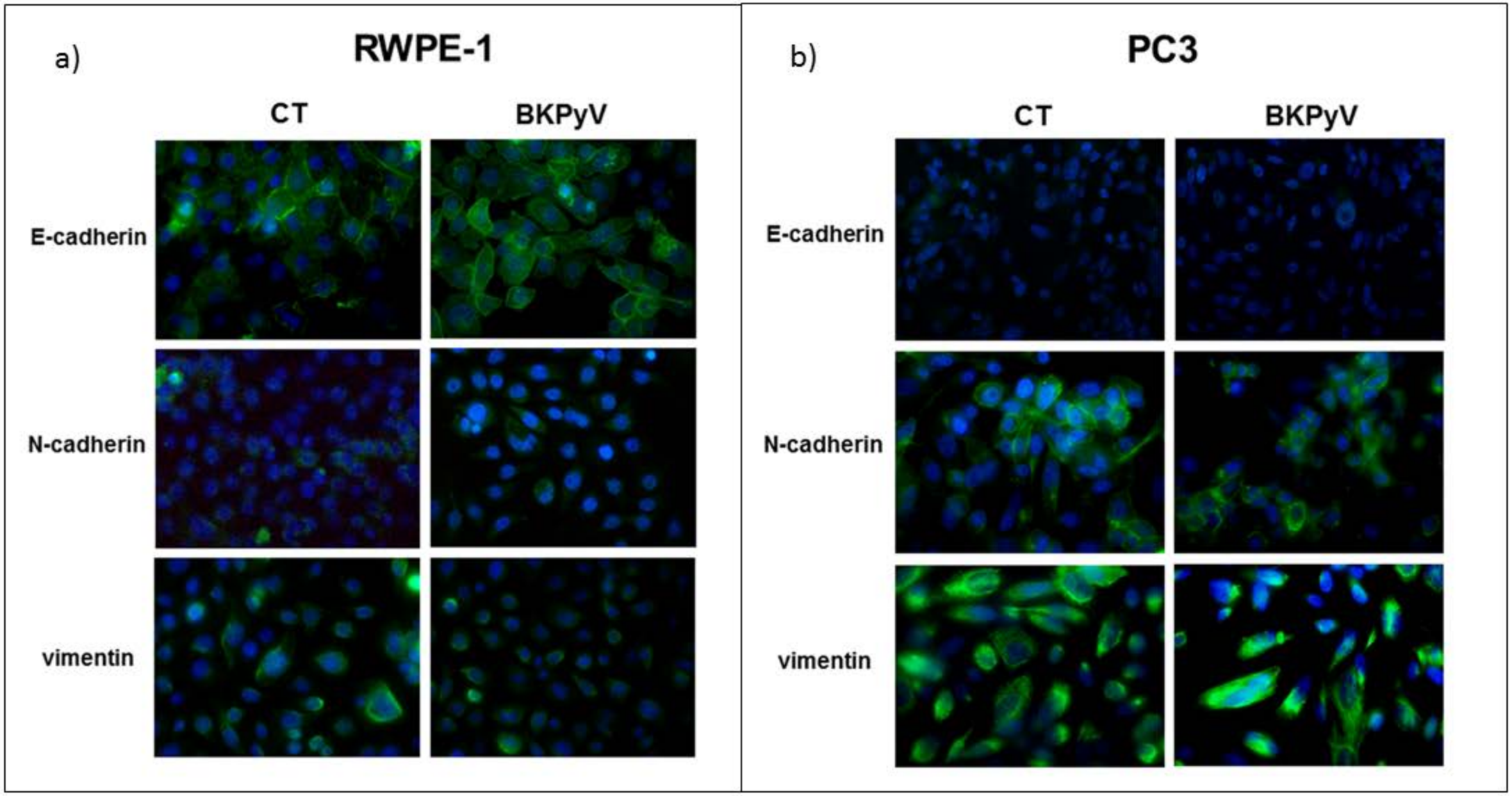
a)
RWPE-1
CT
BKPyV
E-cadherin
N-cadherin
vimentin
b)
PC3
CT
BKPyV
E-cadherin
N-cadherin
vimentin

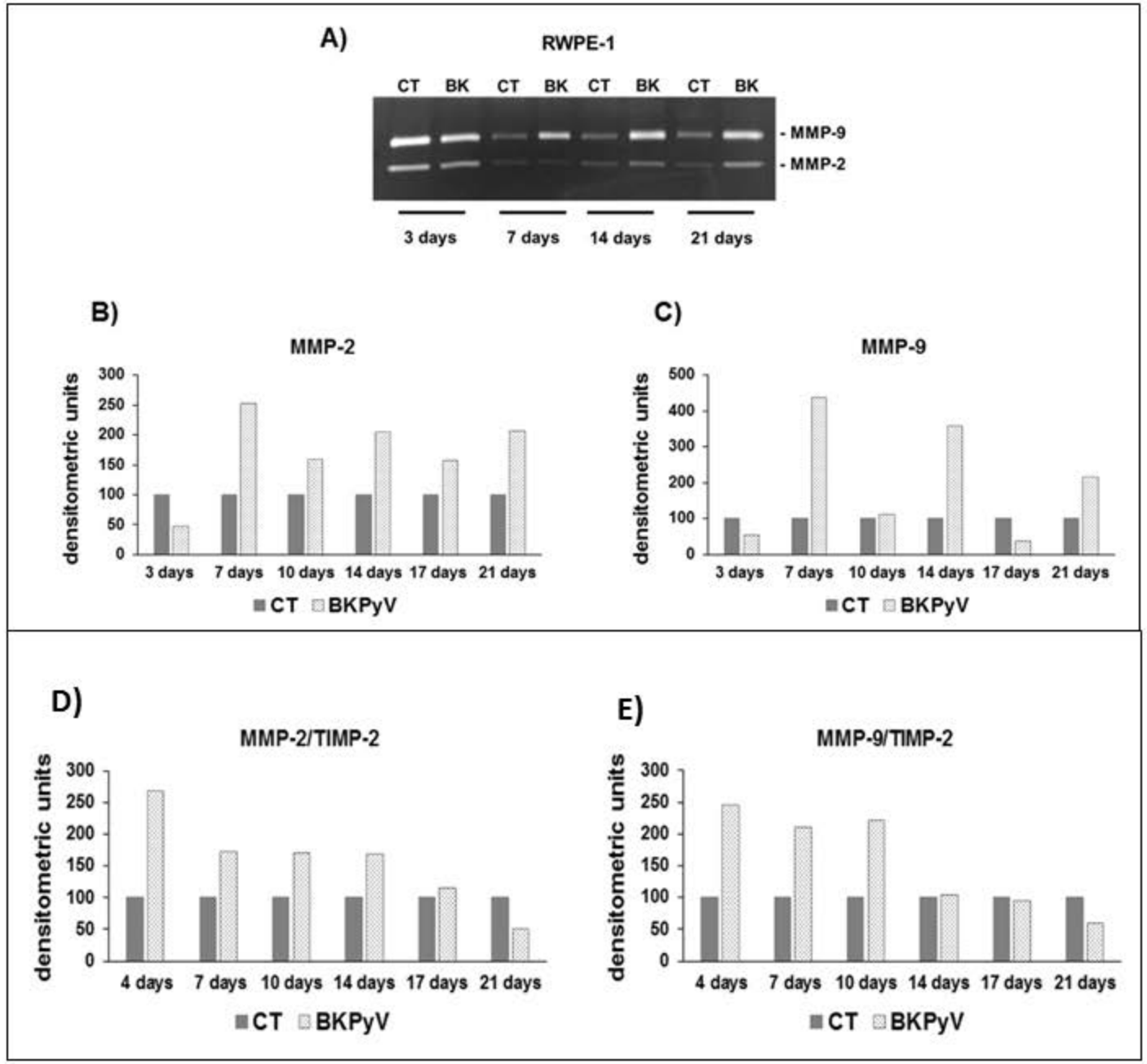
A)
RWPE-1
CT BK CT BK CT BK CT BK
- MMP-9
- MMP-2
3 days
7 days
14 days
21 days
B)
MMP-2
densitometric units
300
250
200
150
100
50
0
3 days 7 days 10 days 14 days 17 days 21 days
CT BKPyV
C)
MMP-9
densitometric units
500
400
300
200
100
0
3 days 7 days 10 days 14 days 17 days 21 days
CT BKPyV
D)
MMP-2/TIMP-2
densitometric units
300
250
200
150
100
50
0
4 days 7 days 10 days 14 days 17 days 21 days
CT BKPyV
E)
MMP-9/TIMP-2
densitometric units
300
250
200
150
100
50
0
4 days 7 days 10 days 14 days 17 days 21 days
CT BKPyV

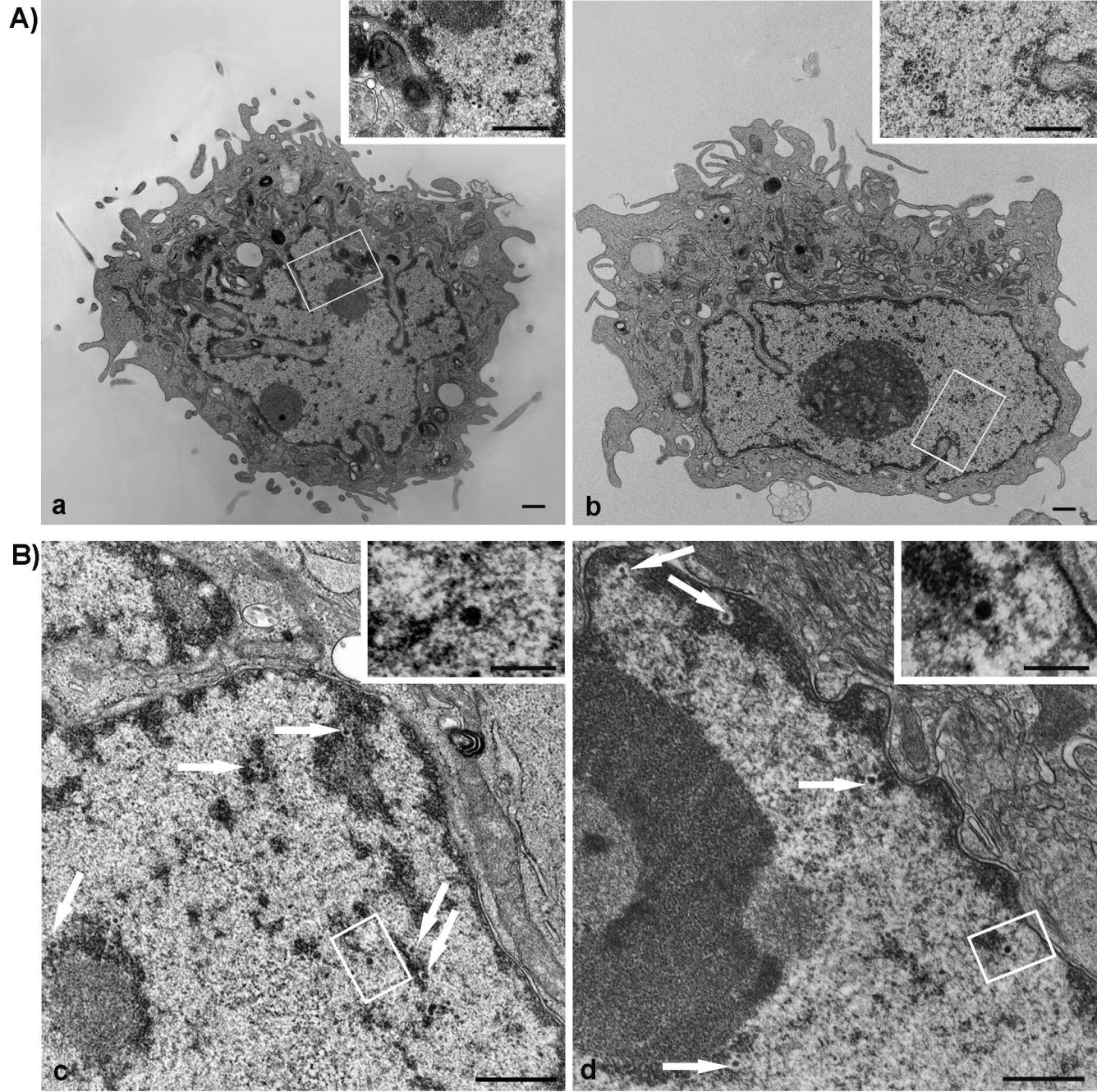
A)
a
b
B)
c
d